Improving Shoreline Forecasting Models with Multi-Objective Genetic Programming

Mahmoud Al Najar
Laboratory of Spatial Geophysics and Oceanography Studies (CNES/CNRS/IRD/UPS)
University of Toulouse
mahmoud.al.najar@legos.obs-mip.fr

Rafael Almar
Laboratory of Spatial Geophysics and Oceanography Studies (CNES/CNRS/IRD/UPS)
University of Toulouse
rafael.almar@ird.fr

Erwin W. J. Bergsma
Earth Observation Lab, The French Space Agency (CNES)
erwin.bergsma@cnes.fr

Jean-Marc Delvit
Earth Observation Lab, The French Space Agency (CNES)
jean-marc.delvit@cnes.fr

Dennis G. Wilson
ISAE-SUPAERO, University of Toulouse
dennis.wilson@isae-supaero.fr

Abstract

Given the current context of climate change and the increasing population densities at coastal zones around the globe, there is an increasing need to be able to predict the development of our coasts. Recent advances in artificial intelligence allow for automatic analysis of observational data. Symbolic Regression (SR) is a type of Machine Learning algorithm that aims to find interpretable symbolic expressions that can explain the relations in the data. In this work, we aim to study the problem of forecasting shoreline change using SR. We make use of Cartesian Genetic Programming (CGP) in order to encode and improve upon ShoreFor, a shoreline prediction model. Coupled with NSGA-II, the CGP individuals are evaluated and selected during evolution according to their predictive skills at five different coastal sites. This work presents a comparison between the CGP-evolved models and the base ShoreFor model. In addition to its ability to produce well-performing models, the work demonstrates the usefulness of CGP as a research tool to gain insight into the behaviors of shorelines at different points around the globe.

1 Introduction

Coasts around the globe are continuously facing natural and anthropogenic pressures. Our knowledge and understanding of the evolution of the coastal zone over time is crucial for a large variety of

This paper is a non-peer reviewed preprint submitted to EarthArXiv. This paper has been submitted to Evolutionary Computation (ECJ).

applications including coastal risk monitoring and management. Shoreline evolution forecasting is an important element in coastal studies that aims to better understand and predict the occurrence and intensity of erosive and accretive forces. Recently, large efforts have been made to understand and predict shoreline evolution due to the rising social, economic and natural pressures such as climate change (Montaño et al., 2020; Church and White, 2006; Nicholls et al., 2014; Reguero et al., 2019). Shoreline change occurs at varying time scales resulting from different natural processes, ranging from small oscillations resulting from individual waves to decadal trends as a response to varying wave climates. At seasonal to interannual scales, cross-shore sediment transport is considered the main driver of shoreline change, while alongshore processes are more relevant at longer timescales (Le Cozannet et al., 2019; Splinter et al., 2014; Toimil et al., 2017).

Symbolic Regression (SR) is a domain of Machine Learning (ML) algorithms that search for symbolic representations of the relationships embedded in the data. Evolutionary algorithms, and specifically Genetic Programming (GP), are often used for SR. GP operates by composing a predefined set of functions in a tree, graph, or other structure; the composition of functions is determined by an evolutionary algorithm. As the optimized model is a functional graph or tree, GP is considered an interpretable ML technique that can be used to derive simple symbolic forms of relationships in data. GP has been demonstrated to be competitive with machine learning approaches such as gradient boosting (La Cava et al., 2021) and has been used in many applications like dimensionality reduction (Uriot et al., 2022), particle physics (Cranmer and Bowman, 2005; Link et al., 2005), quantum computing (Spector et al., 1999; Spector and Klein, 2008), wave characteristic prediction (Goldstein et al., 2013), and water stream-flow forecasting (Makkeasorn et al., 2008).

This work frames the problem of forecasting cross-shore shoreline change as a data-driven symbolic regression task. We experiment on the use of Cartesian Genetic Programming (CGP) and the Non-dominated Sorting Genetic Algorithm II (NSGA-II) to encode and evolve interpretable shoreline change models. To promote model generalization, the evolved models are optimized to maximize prediction accuracy at five different coastal sites from around the globe. Evolution discovers new shoreline forecasting models which outperform existing physical models on the individual sites and also across the five studied sites. We analyze two proposed models which perform well generally to demonstrate their explainability.

We next present an overview of symbolic regression and shoreline change forecasting, with a presentation of the ShoreFor (Davidson et al., 2013) forecasting method used as a baseline model for comparison and improvement in this work. We then present the study sites and datasets used in Section 3. The method, a combination of CGP and NSGA-II adapted for genetic improvement, and the implementation of the ShoreFor model as a CGP graph, are presented in Section 4. Finally, we detail the evolutionary multi-objective optimization on the selected sites in Section 5 and analyze the highest performing models in Section 6, including two generalist models which outperform ShoreFor across the five sites while being simple and interpretable.

2 Related works

2.1 Symbolic Regression

Symbolic regression (SR) is a family of ML algorithms that search for mathematical expressions that best describe the relations between the independent input variables and a dependent output variable. The search space is bounded by a predefined set of components including a set of elementary mathematical operators, constants, and input variables. SR algorithms are particularly interesting as reasearch tools as the outputs of these algorithms are arithmetic expressions rather than sets of coefficients, making them highly interpretable, which allows the practitioner to gain insight into the real-world processes embedded in observed datasets in addition to developing powerful prediction models.

SR algorithms appear in a wide array of applications in the literature. SR was used in (Quade et al., 2016) to predict the dynamics of harmonic and coupled oscillators, as well as the power production of solar panels. In (Udrescu and Tegmark, 2020; Udrescu et al., 2020), a physics-inspired method for symbolic regression based on neural networks is developed and tested on a set of 100 equations from the *Feynman Lectures on Physics*. (Vaddireddy et al., 2020) applies SR to discover hidden physics in a variety of problems using sparse observation data. Multiple works make use of SR to study the nonlinear changes in the properties of materials in response to external factors (Wang et al., 2019b; Weng et al., 2020; Kabliman et al., 2021). We refer the interested reader to (Orzechowski et al., 2018; La Cava et al., 2021) for comprehensive reviews on SR. A common point among the diverse SR literature is the use of GP as one of the main methods for SR.

Despite its adoption in other domains, the use of SR, and GP in particular, remains relatively unexplored in coastal science. Some of the related works in coastal science making use of GP include (Gaur and Deo, 2008), where GP is used to perform real-time wave forecasting and is shown to be a promising tool for coastal prediction studies. In (Kambekar and Deo, 2012), GP was successfully used to perform shore-term forecasting of wave heights based on wind speed and direction, and the evolved models were shown to be applicable over physically-similar but previously-unseen sites. (Passarella et al., 2018) makes use of GP to predict swash zone excursion on sandy beaches. The authors compare their GP-based models to existing literature and show that the GP can be used to develop higher performing predictors while gaining insight into the physical processes, demonstrating the use of GP as a strong data analysis tool.
In (Goldstein et al., 2019), the authors review a large number of ML applications to coastal problems including sediment transport and coastal morphodynamics. Although some works make use of GP, the majority of existing ML-based literature in the domain make use of Artificial Neural Networks and Bayesian Networks in order to learn predictive models from the data. Here, we make use of Cartesian Genetic Programming (CGP) in a multi-objective optimization scheme using the Non-dominated sorting algorithm (NSGA-II) in order to evolve an existing shoreline forecasting model.

2.2 Existing methods in shoreline change forecasting

Three main types of methods have been proposed and discussed in the literature on the topic of forecasting shoreline change (Montaño et al., 2020).
Process-based models include detailed information on the physical processes that happen in the nearshore including wave propagation and dissipation, nearshore currents, sediment transport processes and the resulting changes in the nearshore morphology. These simulated processes are usually coupled through mass and momentum conservation laws. Such models include MIKE 21 (Warren and Bach, 1992), Delft3D (Lesser et al., 2004), ROMS (Warner et al., 2008) and CROCO (Marchesiello et al., 2022). In general, these models are used to model short-term and local events in the nearshore zone and are not considered applicable over larger spatio-temporal scales (Montaño et al., 2020; Davidson, 2021).
Hybrid models are mixed approaches to modelling shoreline change incorporating general physical principles, such as the principle of shoreline equilibrium (Wright et al., 1985), and are calibrated using data-driven approaches (e.g. least-squares-fit). A large number of hybrid models have been developed in the literature (Davidson et al., 2013; Turki et al., 2013; Vitousek et al., 2017; Ibaceta et al., 2022). Compared to process-based models, hybrid models can be used to predict shoreline position over much longer time scales, however they are generally unable to generalize to previously-unseen areas and require site-specific field data for model calibration.
Finally, data-driven techniques rely fully on the available dataset in order to learn the physical relationship between the forcing parameters in the input data and the resulting shoreline change as the output. In (Zeinali et al., 2021; Calkoen et al., 2021), different variants of neural networks are compared with more traditional shoreline forecasting techniques. In both works, neural network-based models demonstrate higher accuracy in their forecasts. In (Montaño et al., 2020), a number of shoreline forecasting techniques, including data-driven, are applied at Tairua in New Zealand in a competition setting. In general, data-driven techniques perform well over familiar conditions and settings, but they fail to generalize to previously-unseen sites and wave conditions and require an extensive dataset for model re-training before application.

2.2.1 ShoreFor

ShoreFor (Davidson et al., 2013) is a shoreline change forecasting model that is built upon the principle of shoreline equilibrium (Wright et al., 1985), where shorelines continuously evolve towards a time-varying equilibrium condition. ShoreFor can be formulated according to Equation 1, where dx/dt is the rate of shoreline change, F is the magnitude of wave forcing, c and b are model free parameters that are optimized using a least-squares-fit minimizing the root-mean-squared-error (RMSE) of the model.

$$\frac{dx}{dt} = c(F^{+} + rF^{-}) + b \tag{1}$$

The wave forcing term F (Equation 2) is expressed in terms of the wave energy flux P and the normalized disequilibrium term $\Delta\Omega/\sigma_{\Delta\Omega}$.

$$F = P^{0.5}\frac{\Delta\Omega}{\sigma_{\Delta\Omega}} \tag{2}$$

ShoreFor defines the beach equilibrium state (Ω_{eq}, Equation 3) as a weighted average of antecedent dimensionless fall velocities where ϕ is a model-free parameter which controls the number of days in the series used to estimate the current equilibrium state.

$$\Omega_{eq} = \frac{\sum_{i=1}^{2\phi} \Omega_i 10^{-i/\phi}}{\sum_{i=1}^{2\phi} 10^{-i/\phi}} \tag{3}$$

Ω, calculated according to Equation 4, represents the rate of sedimentation and is a function of the sediment grain settling velocity w, the breaking wave height $H_{s,b}$ and wave period T_p.

$$\Omega = \frac{H_{s,b}}{wT_p} \tag{4}$$

Disequilibrium, $\Delta\Omega = \Omega_{eq} - \Omega$, is used to partition forcing F into accretion and erosion (F^+, F^-) according to the sign of $\Delta\Omega$. The erosion ratio r (Equation 5) is defined as a ratio between the detrended accretive and erosive wave forcing. It is calculated over the full wave forcing time series and treated as a constant to balance the accretion and erosion terms within the ShoreFor model.

$$r = \left| \frac{\sum_{i=0}^{N} \langle F_i^+ \rangle}{\sum_{i=0}^{N} \langle F_i^- \rangle} \right| \tag{5}$$

ShoreFor has been used in multiple shoreline prediction studies and a number of extensions have been proposed to improve its performance by accounting for shoreline change over different time-scales (Schepper et al., 2021) as well as alongshore sediment transport processes (Tran and Barthélemy, 2020; Tran et al., 2021). We make use of the ShoreFor model as a base for our experiments on the use of CGP for shoreline forecasting in a GI setting, and we highlight the possibility of extending the base CGP-ShoreFor implementation to account for these additional processes.

3 Study zones

Shoreline datasets from five different sites around the globe covering different coastal settings are used in this work. As shown in Figure 1, these sites include the Grand Popo beach in Benin, Gulf of Guinea, in West Africa. Truc Vert beach in the Aquitaine region of France. Narrabeen beach on the coastline of the Sydney metropolitan area, on the eastern coast of Australia. In addtion to two different sites from the USA, Duck NC on the eastern coast, and Torrey Pines on the western coast. A mixture of techniques were used to gather these datasets. Video-derived shoreline time series are used to compose the shoreline time series of Grand Popo and Narrabeen. In-situ GPS surveys were performed to record the shoreline positions of the remaining sites (Duck, Torrey Pines, Truc Vert). Regarding the wave parameters including significant wave height (Hs), peak wave period (Tp), and wave direction (Dir), a mixture of in-situ techniques (wave-bouys) and modelling were used to create the time series over the five sites. These parameters are used to compute the Ω and P time series according to (Davidson et al., 2013). Sea-level anomaly was observed from satellite altimetry over all sites, while river discharge was extracted from a global model hindcast (ISBA-CTRIP) and represents the regional impact of river discharge.
Figure 2 presents the shoreline time series and the associated wave energy flux (P) time series used in this work, and demonstrates the differences in wave forcing and the resulting shoreline behaviors over the five different coastal sites.

4 Methods

To find improved shoreline forecasting models on the five sites, we use Cartesian Genetic Programming, a form of GP which encodes functions as graph. We encode the original ShoreFor model as a GCP graph for automatic improvement. NSGA-II, a genetic algorithm, is then used to improve models over the five sites simultaneously.

4.1 Cartesian Genetic Programming

Cartesian Genetic Programming (CGP) (Miller, 2011) is a form of genetic programming that encodes programs as directed acyclic graphs. An individual CGP graph is composed of three components: input nodes, output nodes and computation nodes. To represent a program as a genome, each node in the graph can be associated with integers corresponding to the function of the node and its inputs; two-arity functions like $x + y$ are most common and used here, so each node is represented

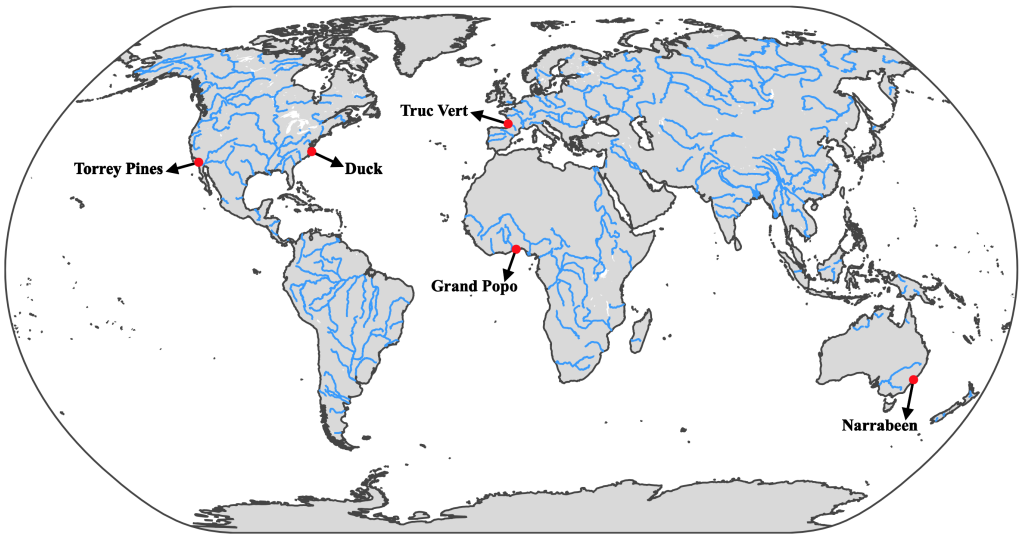

Figure 1: World map highlighting the locations of the five sites included in this study.

by three integers. These integers are optimized by evolution by constructing a graph which connects output nodes to input nodes and evaluating this graph in an objective function. A CGP genome is of fixed size, however the program graph can be of variable size as only a subset of nodes are connected to the output nodes and finally used during evaluation. This allows for flexibility in the number of nodes an individual can use, where nodes that do not contribute to the output are simply ignored during individual evaluation. CGP has been successfully applied to a large number of problems including digital circuit design (Češka et al., 2017), image processing (Sekanina et al., 2011; Harding et al., 2013), computer vision-based applications (Wilson et al., 2018), among others (Miller, 2020). In this work, we use a mostly standard CGP representation with modifications to optimization for NSGA-II and more efficient mutations, and modifications to the function set in order to represent ShoreFor. As in (Al Najar et al., 2022), we employ the following mutation-level constraints: 1) We discard all mutated graphs with direct input-output connections. 2) We ensure that for the same set of random inputs, the outputs produced by parent graph and the mutated graph are different in order to minimze the chances of having behaviorally identical individuals in the population. 3) Since we use a mixed-type version of CGP where both scalar and vector values exist within the computational graph, we add a constraint that discards any mutated graph that outputs scalar values. 4) Finally, we ensure that the size of the output vector is equal to the size of the input time series.

4.2 Encoding ShoreFor in CGP

We encode the ShoreFor model as a CGP individual in order to improve it using evolution. The first population of models is created by randomly mutating the ShoreFor individual, and random genes are used to fill in the inactive nodes. The encoding also informs the inputs available and the function set, as we use functions during search which are necessary to encode the ShoreFor individual.
We first implement equation 3, the Ω_eq time series, by calculating the weight vector $W = 10^{-i/\phi}$, which is computed such that the weighting factor decreases per day i over the number of days ϕ. In order to encode the computation of this weight vector, two inputs and five different functions are required; the inputs are the calibrated ϕ constant and the value of 2ϕ, which specifies the size of the moving window. Given these inputs, we decompose the calculation of W as follows. First, a vector of length 2ϕ with values ranging from 1 to 2ϕ is computed using the $irange$ function. This vector is then simply flipped using the $reverse$ function, to represent the number of days back in history each point in the time series represents. At this point, the vector of i in $10^{-i/\phi}$ is computed. Then, this vector is negated using the $negate$ function and divided by the input constant phi using div, resulting in a vector of values representing $-i/\phi$. This vector is passed to the $tpow$ function ($tpow(x) = 10^x$), obtaining $W = 10^{-i/\phi}$. In order to compute the moving average over the full time series, we make use of the convolution function. We therefore modify the computation of Ω_{eq} as follows: $\Omega_{eq} = conv(\Omega, \frac{10^{-i/\phi}}{\sum_{i=1}^{2\phi} 10^{-i/\phi}})$. The next step in the computational graph is to divide the

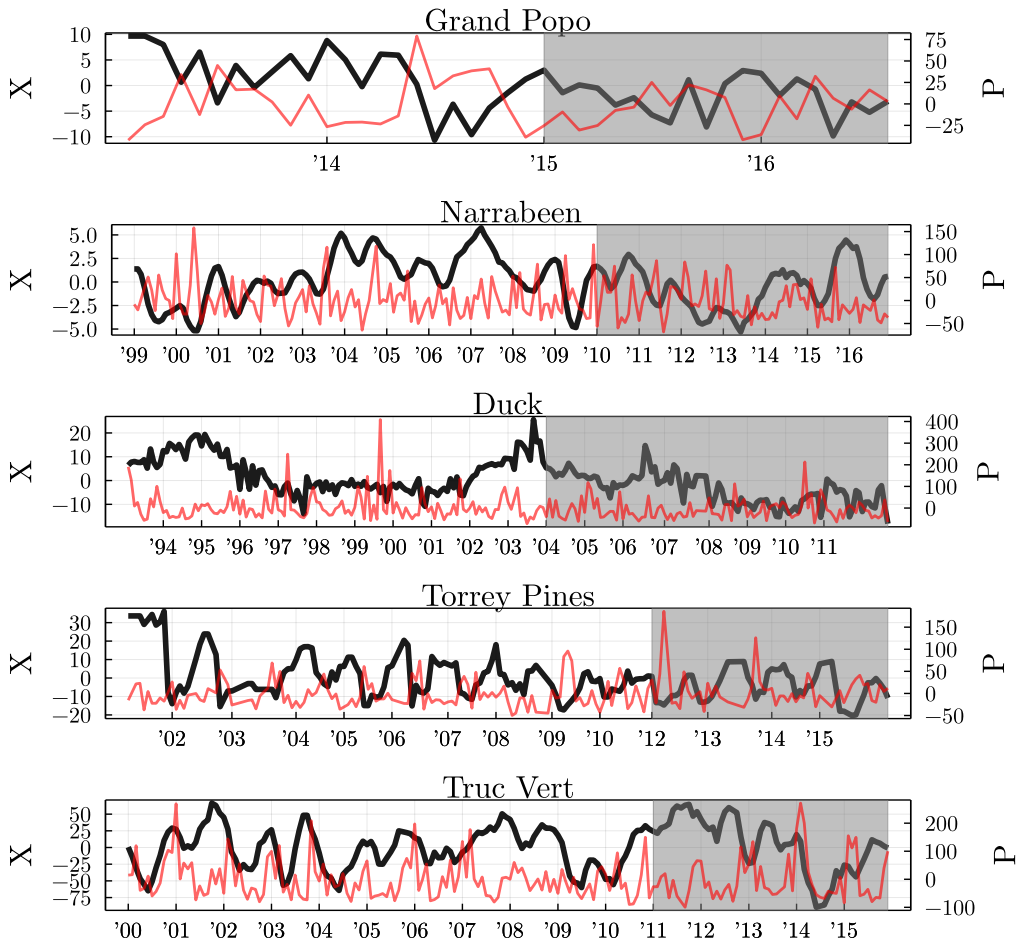

Figure 2: Visualization of the shoreline time series from each of the five sites used in this work. Shoreline location (X) is shown in black. Wave power (P) is shown in red. The shaded area corresponds to the forecast period at each site.

weight vector by the sum of the vector itself to be used as the convolution filter. The graph-form of Equation 3 is shown in Figure 3(left).

The final set of inputs used in our CGP-ShoreFor implementation is described in Table 1. We note that not all inputs included in our implementation are used by the ShoreFor model. These additional inputs are included so that evolution can integrate them into the evolved models.

Input	Description
Ω	Dimensionless fall-velocity time series
P	Wave power time series
ϕ	Pre-calibrated number of days used for the initial ShoreFor model
2ϕ	Used to indicate the size of the weight vector in Equation 3
D*	Wave direction time series
$H_{s,b}$*	Peak breaking wave height
T_p*	Peak wave period
S*	Sea level anomaly
R*	Regional river discharge

Table 1: Inputs to the CGP-ShoreFor model. *Additional inputs that are not used by ShoreFor.

Generally speaking, implementations of CGP require that all input and computed variables are bound to a range of -1 to 1 in order to prevent various computational issues such as the existance

of NaN's or infinities in the computational graph. However, this requirement is difficult to achieve in the case of GI of a physical system of equations due to the lack of true maxima for each input and the use of unbounded functions in the original model. Therefore, we instead choose to handle out-of-bounds computation by penalizing all such individuals by assigning them a fitness value of negative infinity, essentially discarding them from future generations.
After encoding the ShoreFor system of equations as a single CGP genome, the ShoreFor individual can be represented as a graph structure as shown in Figure 3(right).

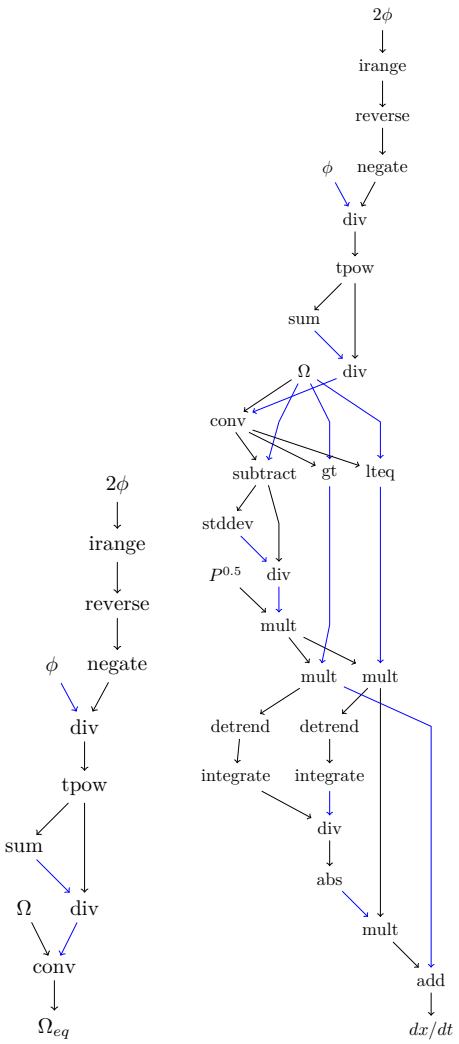

Figure 3: Graph representations of the Ωeq equation (left) and the full ShoreFor system of equations (right).

Currently, the implementation of ShoreFor as a CGP individual assumes that the equations to calculate P and Ω are physical facts and are therefore not included in the evolvable CGP-ShoreFor implementation, but rather passed as pre-calculated time series.

4.3 NSGA-II

NSGA-II is a well-known and widely used multi-objective genetic algorithm that was proposed in (Deb et al., 2002). It makes use of the concept of pareto dominance in order to split a population of models into different performance-based ranks. A crowding distance measure is also used in order to maintain the diversity of population during evolution. At generation G_t, parents (P_t) are selected from the current population using tournament selection and are mutated in order to generate a population of offspring models Q_t. Individuals in Q_t are evaluated according to the user-defined

fitness function, then a combined population R_t is created by merging both P_t and Q_t. R_t is then sorted according based on pareto dominance, as well as the crowding distance in lower-ranks, and the N top-ranking individuals are chosen as the upcoming population. The algorithm is run in a loop until a certain threshold is reached, such as the number of evaluations executed or a predefined fitness threshold. Due to the elitist nature of NSGA-II, top-ranking models are guaranteed to be conserved through the different generations until they are replaced by higher-ranking models. We invite the reader to refer to the original work in (Deb et al., 2002) for further details on the NSGA-II algorithm.
Since it's publication, NSGA-II has been applied to a large variety of multi-objective optimization tasks (Yusoff et al., 2011; Brownlee and Wright, 2015; Delgarm et al., 2016; Wang et al., 2019a; Zhang et al., 2020; Shi et al., 2020). In Kalkreuth et al. (2016), CGP is coupled with a modified version of NSGA-II in order to evolve small mathematical expressions and image processing filters and operators. The proposed modified version of NSGA-II is intended to reduce the number of fitness evaluations needed to obtain a solution. Hilder et al. (2010) presents the first use of a multi-objective fitness function to improve cartesian genetic programming circuits. The authors make use of NSGA-II as a post-processing step to traditional CGP. Functional CGP individuals representing digital circuits are selected at the end of evolution and a pareto front is constructed according to three different criteria. In this work, we make use of NSGA-II with five fitness dimensions in order to rank our CGP individuals during evolution according to their predictive skills at five different coastal sites.

4.4 Fitness evaluation

In this work, we make use of a modified version of the Mielke skill test as proposed in (Duveiller et al., 2016) in order to evaluate the performances of the models. The modified version of the Mielke skill test, formulated as Equation 6, is an extension of the Pearson correlation coefficient (r) that downgrades the value of r according to the bias between the two datasets.

$$\lambda = 1 - \frac{N^{-1}\sum_{i=1}^{N}(o_i - m_i)^2}{\sigma_o^2 + \sigma_m^2 + (\hat{o} - \hat{m})^2} \tag{6}$$

This score is used in order to evaluate the fitness of our CGP individuals over the calibration period during evolution, where the objective is to maximize their Mielke score. We also use it to evaluate the forecast performances of the individuals after evolution as presented in Section 6.

5 Model optimization

In this work, NSGA-II is used to evolve the CGP-encoded individuals. The algorithm is configured according to Table 2 and run for 50 thousand generations. This setup was executed for 50 runs using different random seeds. All runs were found to converge very early on during evolution (within hundreds of generations). After each run, 200 different CGP individuals are recorded representing the final generation from that run. The final generations from all runs are grouped into a single merged population of 10000 individuals and evaluated using the calibration and forecast datasets. Tables 3 and 4 document the different functions used in this work, representing the function set used by the genetic algorithm during evolution.

Parameter	Value
Population size	200
N offsprings	200
Mutation rate	0.1
Output mutation rate	0.3
Rows	1
Columns	50

Table 2: Evolutionary configuration used throughout this work.

In the following section, we present the results of these experiments by discussing the merged population as a whole, and then by evaluating the performance of a small number of evolved individuals.

5.1 Evolution

Figures 4 and 5 visualize the performances of the resulting merged population over the calibration and forecast periods. Most models are able achieve a high score over the calibration set, while their performance during the forecast period varies between the different sites.
In Figure 4, we sort our individuals according to their average Mielke skill score over the 5 sites during the calibration period; while Figure 5 visualizes the same result when sorted according to the mean score over the forecast period. Interestingly, we find that the highest-performing individuals over the calibration period are not necessarily the best-performing models during the forecast period, indicating the tendency of the models to overfit to the calibration time series during evolution.

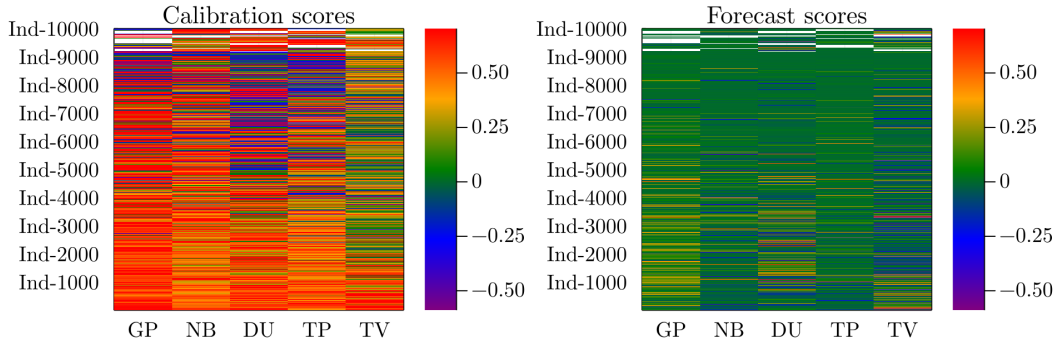

Figure 4: Merged population - sorted by mean Mielke score over the calibration period. The color-scale corresponds to the Mielke score.

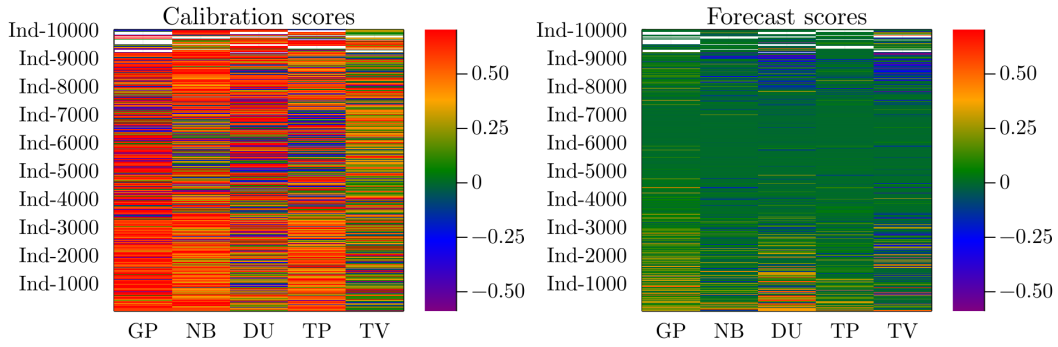

Figure 5: Merged population - sorted by mean Mielke score over the forecast period. The color-scale corresponds to the Mielke score.

For the purpose of this work, we make use of the forecast performance in order to select our highest-performing individuals for further analysis. In the coming section, models are chosen according to two different criteria: site experts are selected according to their forecast performance at a specific site, and are expected to work best at that single site only, whereas generalist-models are selected according to their mean Mielke forecast skill over the 5 different sites with the aim of finding a single model that can perform well over all sites.

6 Model analysis

We now present and analyze the highest-performing models generated by CGP and NSGA-II using ShoreFor as a starting point for evolution. For each site, we present the performances of two site experts, selected per-site, and two generalist models, selected over all five sites, and we compare them to the ground truth data as well as the baseline ShoreFor model. Results on the calibration data used during evolution are presented in 6 and results on the forecast data are shown in 7. Furthermore, in order to have a deeper understanding of model performance, we evaluate the performances of our models over isolated trends of different temporal scales in both the ground truth and predicted time series. This is done using a running mean filter with varying window sizes corresponding to the target time scale, and a pass-band filter to isolate those time scales.

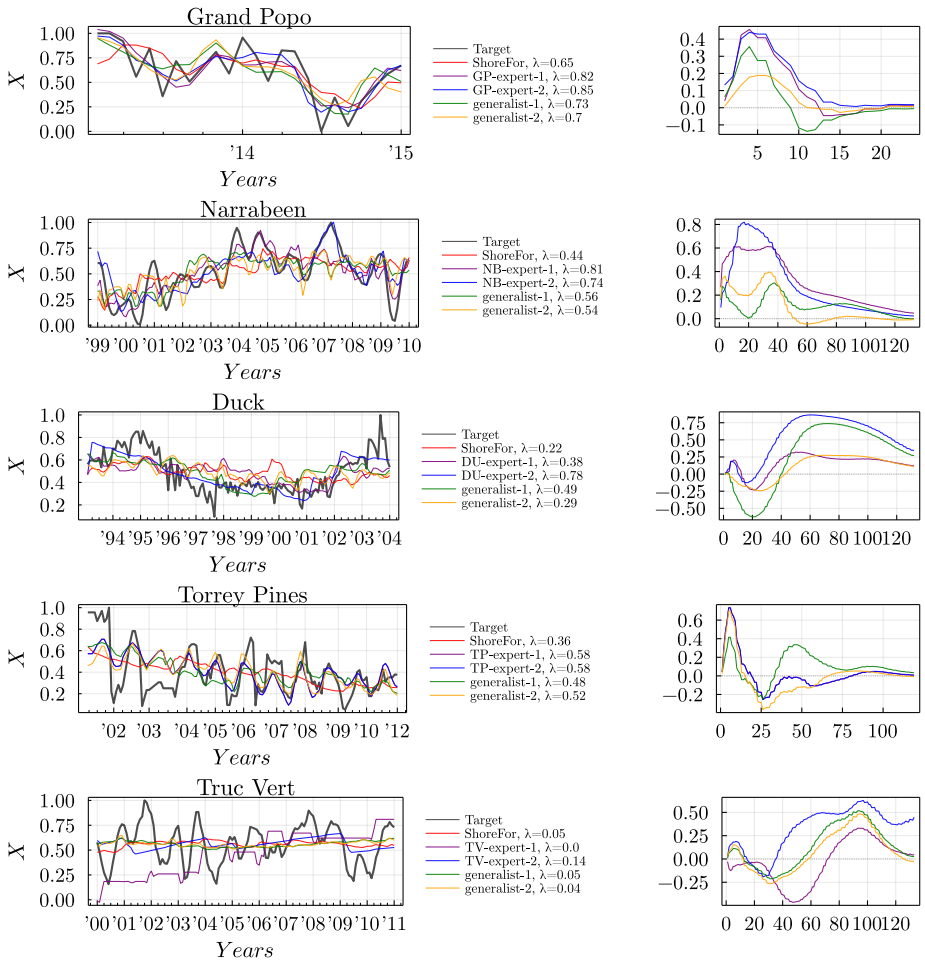

Figure 6: Calibration performances on the five sites (left) and the difference in the Mielke skill score at different time scales compared to the performance of ShoreFor at that time scale ($Y = 0$ represents ShoreFor and the X axis corresponds to the number of months at the evaluated time scale).

All evolved models are able to achieve a higher Mielke skill score over the calibration period compared to the ShoreFor model across the five sites. The main improvement over ShoreFor occurs over relatively shorter-term variations, around five months, as indicated in Figure 6.

On the Grand Popo site, the expert models achieve a 20% gain over ShoreFor on the forecast period. The GP-expert-1 model shows an improvement in performance over all time scales except over shorter-term variations (1-4 months), whereas GP-expert-2 achieves a higher skill score over a single dominant time scale (4-12 months). The generalist models are competitive with ShoreFor while having different behavior, both underperforming at short timescales but improving for longer timescales.

On the Narrabeen dataset, all CGP models achieve a higher Mielke score over both the calibration and forecast periods. Compared to the results at Narrabeen presented in the original ShoreFor work (Davidson et al., 2013), the base ShoreFor model achieves a much lower skill score over the forecast period. We presume that this difference is due to the use of a lower frequency in the dataset; we note that ShoreFor showed high sensitivity to the specific calibration and forecast periods it was applied at. Compared to ShoreFor, the NB-expert models demonstrate a significant improvement during the forecast period, while the two generalist models show a slight improvement.

At Duck, all evolved models show a similar behavior of achieving superior Mielke skill at long time scales, while their performance varies at shorter time scales compared to ShoreFor. All models achieve a higher Mielke skill over both the calibration and forecast periods except for generalist-2.

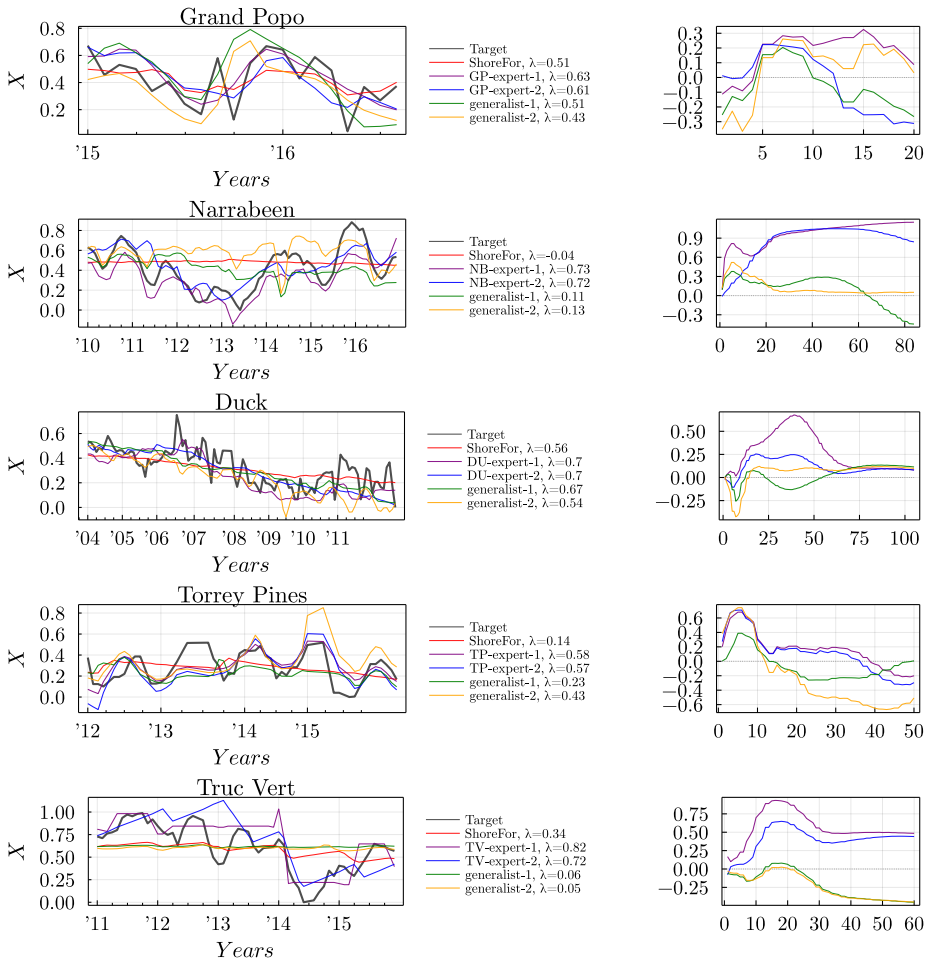

Figure 7: Forecast performances on the five sites (left) and the difference in the Mielke skill score at different time scales compared to the performance of ShoreFor at that time scale ($Y = 0$ represents ShoreFor and the X axis corresponds to the number of months at the evaluated time scale).

Compared to ShoreFor, generalist-2 has a lower score by 0.02 using the raw model output, while its performance shows a consistent improvement at longer time scales.

Similarly, on the Torrey Pines dataset, the evolved models improve on ShoreFor on the calibration and forecast data; specifically, they capture the strong seasonal cycle better in addition to the long term trend in shoreline position, while ShoreFor appears to capture the long term trend only. All models achieve higher skill score using the raw model output compared to ShoreFor, and they show a sharp increase in performance at shorter time scales, while the generalist models show a decrease in performance at longer scales.

At Truc Vert, all models fail to produce a reliable forecast of the shoreline position. Compared to ShoreFor, the generalist models achieve equivalent performance over the calibration period and are worse at the forecast period; as discussed in Section 5.1, models that show high Mielke skill during the calibration period were not necessarily well-performing at the forecast period. While the models presented here are selected based on their forecast skill.

Overall, the expert models chosen for each site demonstrate large improvements over ShoreFor and high correlation with the ground truth forecast data, on which they were not trained. The generalist models perform less well overall, but show a consistent improvement over ShoreFor. While specialist models could be trained for a specific site, offering more accurate predictions, a general model of shoreline change can be applied globally. We now evaluate the two selected generalist models to better understand their differences from ShoreFor.

6.1 Evolved graphs

Figure 8 presents the graph representation of the generalist models discussed in the previous section. Both can also be represented by a system of a equations; the generalist 1 model is equivalent to

$$\frac{dx}{dt} = \begin{cases} \frac{1}{2}\bar{P}^{0.5}\frac{d}{dt}\sqrt{\frac{\phi^2}{2} + \frac{1}{4}(R-\Omega)^2 + S^2}, & \text{if } S \geq P^{0.5} + \Omega \\ 0, & \text{otherwise} \end{cases} \tag{7}$$

and the generalist 2 model to

$$\frac{dx}{dt} = P^{\frac{R}{2}}\frac{d}{dt}10^S \tag{8}$$

We first note that both models differ largely from the original ShoreFor model. While the fall-velocity Ω is used, there is no calculation of an equilibrium term Ω_{eq}, and the wave energy flux P is used directly to calculate $\frac{dx}{dt}$, as opposed to calculating accretive and erosive wave forcing terms F. The combination of information not used in ShoreFor, sea level anomaly S and river discharge R, instead determines the influence of wave power on shoreline change. While it is notable that wave power is the primary driver in both evolved models and in ShoreFor, these evolved models offer a different perspective on the relationship between sea level, river discharge, wave power, and shoreline change.

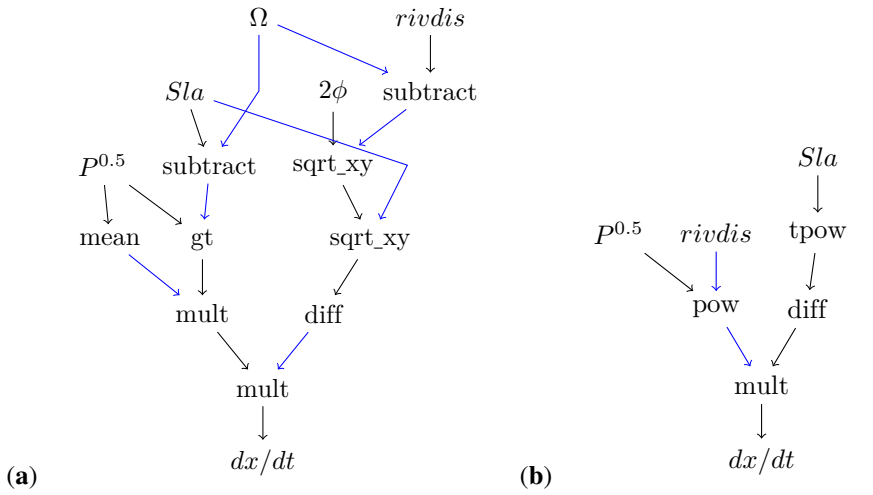

Figure 8: The (a) generalist-1 and (b) generalist-2 models produced by CGP and NSGA-II using ShoreFor as the starting point for evolution.

7 Discussion

As presented in Figures 4 and 5, we found a large discrepancy in model performance between the calibration and forecast periods. This discrepancy can be attributed to over fitting, a common issue encountered with ML models, including GP, where the models learn to replicate the target training data during evaluation, thereby achieving high performance during training without learning the actual underlying relationships embedded in the training dataset. A possible future direction for this work would be to include the Random Sampling Technique (RST) in the evaluation procedure, where only a random subset of the training dataset is used to compute the fitness of individuals at each generation. RST was first proposed in (Gathercole and Ross, 1994) in order to reduce the computational resources required to run GP. Later works demonstrated promising results on the use of RST as a method for improving model generalization in GP (Langdon, 2011; Liu and Khoshgoftaar, 2004; Gonçalves et al., 2012). In the context of this work, RST could be used to select random periods from each time series in order to test model performance during evolution, taking into account the physical signification of the selected periods and their lengths.

Another future direction would be to include shoreline data from Satellite Image Time Series datasets in order to enlarge the coverage of the different sites into coastal zones. The availability of such a dataset would allow for the use of a more globally-representative set of coastal zones to

be used for calibration during evolution. It would also allow for a more exhaustive set of test areas after evolution. We believe that such modifications would greatly increase the algorithm's ability to produce more robust generalist models.
An interesting pattern found during this work is the tendency of the evolved models to degrade the performance of the baseline ShoreFor model at certain time scales (see Figures 6 and 7). One possible way to overcome this degradation would be to set the different time scales (event-scale, seasonal, interannual, decadal) as the objectives for evolution.
Furthermore, this work did not explore the effects of different CGP mutation schemes such as node addition and deletion, in addition to different crossover operations. However, we believe that it could be interesting to explore such operations, especially considering the possibility of including other shoreline forecasting systems into the initial gene-pool of the algorithm.

8 Conclusion

In this work, we have presented our experiments on the use of CGP and NSGA-II in order to evolve a pre-established shoreline forecasting model, ShoreFor. CGP was used in order to encode the ShoreFor system of equations into a format that can be evolved using evolutionary algorithms. During evolution, NSGA-II is employed in order to maintain a pareto-front of optimal solutions according to their performances at five different coastal points from around the globe.
On a population-level, a discrepancy was found between the training and test performances of the evolved models. We believe that the inclusion of additional coastal sites in addition to longer shoreline time series would allow for more sophisticated experimentation on the use of the Random Sampling Technique to increase model generalization.
The evolved models were presented from two different perspectives. Expert models are site-specific experts that are selected according to the highest forecast score at a specific site. These models were found to achieve a higher skill score compared to the baseline ShoreFor model over all sites, during both the calibration and forecast periods. On the other hand, generalist models are selected according to their average forecast skill score over the five different objectives. The generalist models achieve similar or higher performance than that of ShoreFor over four of the five sites used in this work.
Overall, the results presented in this work are a strong motivation for further study on the use of genetic programming and multi-objective genetic algorithms in shoreline forecasting studies due to the wide potential applicability of the evolved models and their interpretability as ordinary systems of equations.

Appendix A Function set

Function	Operation
abs	$\lvert x \rvert$
sqrt	$\sqrt{x}$
sin	$\sin x$
cos	$\cos x$
negate	$-x$
tpow	10^x
nop	x
add	$x + y$
subtract	$x - y$
mult	$x * y$
div	$x \div y$
pow	x^y
sqrt_xy	$\sqrt{x^2 + y^2}$
lteq	$x <= y$
gt	$x > y$

Table 3: The set of scalar operations included in the GA's function set.

Function	Operation
diff	$x_i = x_i - x_{i-1}$
sum	$\sum_{i=1}^{n} x$
stddev	σx
detrend	$\langle x \rangle$
integrate*	$\int_a^b f(x)dx \approx \sum_{i=1}^{n} \frac{f(x_{i-1})+f(x_i)}{2} \Delta x_i$
mean	$\frac{1}{n} \sum_{i=1}^{n} x$
reverse	$reverse(x)$
irange	$[1, 2, 3...n], n = length(x)$
conv	$conv(x, y)$

Table 4: The set of vector operations included in the GA's function set. * Assuming a constant time step in the time series.

References

Al Najar, M., Almar, R., Bergsma, E. W. J., Delvit, J.-M., and Wilson, D. G. (2022). Genetic improvement of shoreline evolution forecasting models. In *Proceedings of the Genetic and Evolutionary Computation Conference Companion*, GECCO '22, page 1916–1923, New York, NY, USA. Association for Computing Machinery.

Brownlee, A. E. and Wright, J. A. (2015). Constrained, mixed-integer and multi-objective optimisation of building designs by nsga-ii with fitness approximation. *Applied Soft Computing*, 33:114–126.

Calkoen, F., Luijendijk, A., Rivero, C. R., Kras, E., and Baart, F. (2021). Traditional vs. machine-learning methods for forecasting sandy shoreline evolution using historic satellite-derived shorelines. *Remote Sensing*, 13(5):934.

Češka, M., Matyáš, J., Mrazek, V., Sekanina, L., Vasicek, Z., and Vojnar, T. (2017). Approximating complex arithmetic circuits with formal error guarantees: 32-bit multipliers accomplished. In *2017 IEEE/ACM International Conference on Computer-Aided Design (ICCAD)*, pages 416–423. IEEE.

Church, J. A. and White, N. J. (2006). A 20th century acceleration in global sea-level rise. *Geophysical research letters*, 33(1).

Cranmer, K. and Bowman, R. S. (2005). Physicsgp: A genetic programming approach to event selection. *Computer Physics Communications*, 167(3):165–176.

Davidson, M. (2021). Forecasting coastal evolution on time-scales of days to decades. *Coastal Engineering*, 168:103928.

Davidson, M., Splinter, K., and Turner, I. (2013). A simple equilibrium model for predicting shoreline change. *Coastal Engineering*, 73:191–202.

Deb, K., Pratap, A., Agarwal, S., and Meyarivan, T. (2002). A fast and elitist multiobjective genetic algorithm: Nsga-ii. *IEEE transactions on evolutionary computation*, 6(2):182–197.

Delgarm, N., Sajadi, B., Delgarm, S., and Kowsary, F. (2016). A novel approach for the simulation-based optimization of the buildings energy consumption using nsga-ii: Case study in iran. *Energy and Buildings*, 127:552–560.

Duveiller, G., Fasbender, D., and Meroni, M. (2016). Revisiting the concept of a symmetric index of agreement for continuous datasets. *Scientific reports*, 6(1):1–14.

Gathercole, C. and Ross, P. (1994). Dynamic training subset selection for supervised learning in genetic programming. In *International Conference on Parallel Problem Solving from Nature*, pages 312–321. Springer.

Gaur, S. and Deo, M. (2008). Real-time wave forecasting using genetic programming. *Ocean engineering*, 35(11-12):1166–1172.

Goldstein, E. B., Coco, G., and Murray, A. B. (2013). Prediction of wave ripple characteristics using genetic programming. *Continental Shelf Research*, 71:1–15.

Goldstein, E. B., Coco, G., and Plant, N. G. (2019). A review of machine learning applications to coastal sediment transport and morphodynamics. *Earth-science reviews*, 194:97–108.

Gonçalves, I., Silva, S., Melo, J. B., and Carreiras, J. (2012). Random sampling technique for overfitting control in genetic programming. In *European Conference on Genetic Programming*, pages 218–229. Springer.

Harding, S., Leitner, J., and Schmidhuber, J. (2013). Cartesian genetic programming for image processing. In *Genetic programming theory and practice X*, pages 31–44. Springer.

Hilder, J., Walker, J. A., and Tyrrell, A. (2010). Use of a multi-objective fitness function to improve cartesian genetic programming circuits. In *2010 NASA/ESA Conference on Adaptive Hardware and Systems*, pages 179–185. IEEE.

Ibaceta, R., Splinter, K. D., Harley, M. D., and Turner, I. L. (2022). Improving multi-decadal coastal shoreline change predictions by including model parameter non-stationarity. *Frontiers in Marine Science*, 9:1012041.

Kabliman, E., Kolody, A. H., Kronsteiner, J., Kommenda, M., and Kronberger, G. (2021). Application of symbolic regression for constitutive modeling of plastic deformation. *Applications in Engineering Science*, 6:100052.

Kalkreuth, R., Rudolph, G., and Krone, J. (2016). More efficient evolution of small genetic programs in cartesian genetic programming by using genotypie age. In *2016 IEEE Congress on Evolutionary Computation (CEC)*, pages 5052–5059. IEEE.

Kambekar, A. and Deo, M. (2012). Wave prediction using genetic programming and model trees. *Journal of Coastal Research*, 28(1):43–50.

La Cava, W., Orzechowski, P., Burlacu, B., de Franca, F. O., Virgolin, M., Jin, Y., Kommenda, M., and Moore, J. H. (2021). Contemporary symbolic regression methods and their relative performance. In *Thirty-fifth Conference on Neural Information Processing Systems Datasets and Benchmarks Track (Round 1)*.

Langdon, W. (2011). Minimising testing in genetic programming. *RN*, 11(10):1.

Le Cozannet, G., Bulteau, T., Castelle, B., Ranasinghe, R., Wöppelmann, G., Rohmer, J., Bernon, N., Idier, D., Louisor, J., and Salas-y Mélia, D. (2019). Quantifying uncertainties of sandy shoreline change projections as sea level rises. *Scientific reports*, 9(1):1–11.

Lesser, G. R., Roelvink, J. v., van Kester, J. T. M., and Stelling, G. (2004). Development and validation of a three-dimensional morphological model. *Coastal engineering*, 51(8-9):883–915.

Link, J., Yager, P., Anjos, J., Bediaga, I., Castromonte, C., Göbel, C., Machado, A., Magnin, J., Massafferri, A., De Miranda, J., et al. (2005). Application of genetic programming to high energy physics event selection. *Nuclear Instruments and Methods in Physics Research Section A: Accelerators, Spectrometers, Detectors and Associated Equipment*, 551(2-3):504–527.

Liu, Y. and Khoshgoftaar, T. (2004). Reducing overfitting in genetic programming models for software quality classification. In *Eighth IEEE International Symposium on High Assurance Systems Engineering, 2004. Proceedings.*, pages 56–65. IEEE Computer Society.

Makkeasorn, A., Chang, N.-B., and Zhou, X. (2008). Short-term streamflow forecasting with global climate change implications–a comparative study between genetic programming and neural network models. *Journal of Hydrology*, 352(3-4):336–354.

Marchesiello, P., Chauchat, J., Shafiei, H., Almar, R., Benshila, R., Dumas, F., and Debreu, L. (2022). 3d wave-resolving simulation of sandbar migration. *Ocean Modelling*, page 102127.

Miller, J. F. (2011). Cartesian genetic programming. In *Cartesian Genetic Programming*, pages 17–34. Springer.

Miller, J. F. (2020). Cartesian genetic programming: its status and future. *Genetic Programming and Evolvable Machines*, 21(1):129–168.

Montaño, J., Coco, G., Antolínez, J. A., Beuzen, T., Bryan, K. R., Cagigal, L., Castelle, B., Davidson, M. A., Goldstein, E. B., Ibaceta, R., et al. (2020). Blind testing of shoreline evolution models. *Scientific reports*, 10(1):1–10.

Nicholls, R. J., Hanson, S. E., Lowe, J. A., Warrick, R. A., Lu, X., and Long, A. J. (2014). Sea-level scenarios for evaluating coastal impacts. *Wiley Interdisciplinary Reviews: Climate Change*, 5(1):129–150.

Orzechowski, P., La Cava, W., and Moore, J. H. (2018). Where are we now? a large benchmark study of recent symbolic regression methods. In *Proceedings of the Genetic and Evolutionary Computation Conference*, pages 1183–1190.

Passarella, M., Goldstein, E. B., De Muro, S., and Coco, G. (2018). The use of genetic programming to develop a predictor of swash excursion on sandy beaches. *Natural Hazards and Earth System Sciences*, 18(2):599–611.

Quade, M., Abel, M., Shafi, K., Niven, R. K., and Noack, B. R. (2016). Prediction of dynamical systems by symbolic regression. *Physical Review E*, 94(1):012214.

Reguero, B. G., Losada, I. J., and Méndez, F. J. (2019). A recent increase in global wave power as a consequence of oceanic warming. *Nature communications*, 10(1):1–14.

Schepper, R., Almar, R., Bergsma, E., de Vries, S., Reniers, A., Davidson, M., and Splinter, K. (2021). Modelling cross-shore shoreline change on multiple timescales and their interactions. *Journal of Marine Science and Engineering*, 9(6):582.

Sekanina, L., Harding, S. L., Banzhaf, W., and Kowaliw, T. (2011). Image processing and cgp. In *Cartesian genetic programming*, pages 181–215. Springer.

Shi, S., Ge, Y., Chen, L., and Feng, H. (2020). Four-objective optimization of irreversible atkinson cycle based on nsga-ii. *Entropy*, 22(10):1150.

Spector, L., Barnum, H., Bernstein, H. J., and Swamy, N. (1999). Quantum computing applications of genetic programming. *Advances in genetic programming*, 3:135–160.

Spector, L. and Klein, J. (2008). Machine invention of quantum computing circuits by means of genetic programming. *AI EDAM*, 22(3):275–283.

Splinter, K. D., Turner, I. L., Davidson, M. A., Barnard, P., Castelle, B., and Oltman-Shay, J. (2014). A generalized equilibrium model for predicting daily to interannual shoreline response. *Journal of Geophysical Research: Earth Surface*, 119(9):1936–1958.

Toimil, A., Losada, I. J., Camus, P., and Díaz-Simal, P. (2017). Managing coastal erosion under climate change at the regional scale. *Coastal Engineering*, 128:106–122.

Tran, Y. H. and Barthélemy, E. (2020). Combined longshore and cross-shore shoreline model for closed embayed beaches. *Coastal Engineering*, 158:103692.

Tran, Y. H., Marchesiello, P., Almar, R., Ho, D. T., Nguyen, T., Thuan, D. H., and Barthélemy, E. (2021). Combined longshore and cross-shore modeling for low-energy embayed sandy beaches. *Journal of Marine Science and Engineering*, 9(9):979.

Turki, I., Medina, R., Coco, G., and Gonzalez, M. (2013). An equilibrium model to predict shoreline rotation of pocket beaches. *Marine Geology*, 346:220–232.

Udrescu, S.-M., Tan, A., Feng, J., Neto, O., Wu, T., and Tegmark, M. (2020). Ai feynman 2.0: Pareto-optimal symbolic regression exploiting graph modularity. *Advances in Neural Information Processing Systems*, 33:4860–4871.

Udrescu, S.-M. and Tegmark, M. (2020). Ai feynman: A physics-inspired method for symbolic regression. *Science Advances*, 6(16):eaay2631.

Uriot, T., Virgolin, M., Alderliesten, T., and Bosman, P. A. (2022). On genetic programming representations and fitness functions for interpretable dimensionality reduction. In *Proceedings of the Genetic and Evolutionary Computation Conference*, pages 458–466.

Vaddireddy, H., Rasheed, A., Staples, A. E., and San, O. (2020). Feature engineering and symbolic regression methods for detecting hidden physics from sparse sensor observation data. *Physics of Fluids*, 32(1):015113.

Vitousek, S., Barnard, P. L., Limber, P., Erikson, L., and Cole, B. (2017). A model integrating longshore and cross-shore processes for predicting long-term shoreline response to climate change. *Journal of Geophysical Research: Earth Surface*, 122(4):782–806.

Wang, S., Zhao, D., Yuan, J., Li, H., and Gao, Y. (2019a). Application of nsga-ii algorithm for fault diagnosis in power system. *Electric Power Systems Research*, 175:105893.

Wang, Y., Wagner, N., and Rondinelli, J. M. (2019b). Symbolic regression in materials science. *MRS Communications*, 9(3):793–805.

Warner, J. C., Sherwood, C. R., Signell, R. P., Harris, C. K., and Arango, H. G. (2008). Development of a three-dimensional, regional, coupled wave, current, and sediment-transport model. *Computers & geosciences*, 34(10):1284–1306.

Warren, I. and Bach, H. (1992). Mike 21: a modelling system for estuaries, coastal waters and seas. *Environmental Software*, 7(4):229–240.

Weng, B., Song, Z., Zhu, R., Yan, Q., Sun, Q., Grice, C. G., Yan, Y., and Yin, W.-J. (2020). Simple descriptor derived from symbolic regression accelerating the discovery of new perovskite catalysts. *Nature communications*, 11(1):1–8.

Wilson, D. G., Cussat-Blanc, S., Luga, H., and Miller, J. F. (2018). Evolving simple programs for playing atari games. In *Proceedings of the Genetic and Evolutionary Computation Conference*, pages 229–236.

Wright, L. D., Short, A. D., and Green, M. (1985). Short-term changes in the morphodynamic states of beaches and surf zones: an empirical predictive model. *Marine geology*, 62(3-4):339–364.

Yusoff, Y., Ngadiman, M. S., and Zain, A. M. (2011). Overview of nsga-ii for optimizing machining process parameters. *Procedia Engineering*, 15:3978–3983.

Zeinali, S., Dehghani, M., and Talebbeydokhti, N. (2021). Artificial neural network for the prediction of shoreline changes in narrabeen, australia. *Applied Ocean Research*, 107:102362.

Zhang, L., Chen, L., Xia, S., Ge, Y., Wang, C., and Feng, H. (2020). Multi-objective optimization for helium-heated reverse water gas shift reactor by using nsga-ii. *International Journal of Heat and Mass Transfer*, 148:119025.